The development of First-Flex, a new flexible Optical Solar Reflector

Sandro Mengali[a], Mirko Simeoni[b], Alessandro Urbani[c] and Matteo Gaspari[d]
CREO, L'Aquila, 67100, Italy

Michele Magistretti[e] and Cesare Sabato[f]
ODL, Brembate di Sopra, 24030, Italy

Marco Ivagnes[g], Fabrizio Poscente[h] and Francesco Di Marcantonio[i]
Thales Alenia Space, L'Aquila, 67100, Italy

and

Marco Gottero[j], Marina Gentile[k], Federica Tessarin[l], Albino Quaranta[m] and Andrea Ferrero[n]
Thales Alenia Space, Torino, 10146, Italy

First-Flex is a new type of flexible Optical Solar Reflector (OSR) made of a multi-layer coating on the space facing surface of polyimide tape. First-Flex is designed to combine the high performance and durability of quartz OSRs with the easy handling of Second Surface Mirrors. This paper reports on the results of a test campaign aimed at qualifying First-Flex for a 15-years mission in Geostationary Earth Orbit. Radiation test conditions are discussed in some details, and it is shown that Total Ionization Doses are at least equivalent to a Life Test both in the coating and in the transfer tape. The main finding is that samples pass qualification and have solar absorptance $\alpha \leq 0.12$ and IR emittance ≥ 0.79 at the end of the test sequence, with a performance degradation of only 2% respect to values at the Beginning of Life.

Nomenclature

α = Solar Absorptance

[a] Director, Consorzio CREO, SS 17 località boschetto snc, 67100 L'Aquila, Italy
[b] Head Technology Lab, Consorzio CREO, SS 17 località boschetto snc, 67100 L'Aquila, Italy
[c] Researcher, Consorzio CREO, SS 17 località boschetto snc, 67100 L'Aquila, Italy
[d] Researcher, Consorzio CREO, SS 17 località boschetto snc, 67100 L'Aquila, Italy
[e] Technical Director, ODL Srl, Via G. Terzi di S. Agata 17, 24030 Brembate di sopra (BG), Italy
[f] Chief Executive Officer, ODL Srl, Via G. Terzi di S. Agata17, 24030 Brembate di sopra (BG), Italy
[g] Industrial Architect, Thales Alenia Space, Via Cassini 6, 67100 L'Aquila, Italy
[h] Head of Mechanical Technology and Processes Engineering Dpt, Thales Alenia Space, Via Cassini 6, 67100 L'Aquila, Italy
[i] Mechanical Technology and Processes Engineering Dpt, Thales Alenia Space, Via Cassini 6, 67100 L'Aquila, Italy
[j] Head of Passive Thermal Design Unit, Thermal & Environmental Control and Propulsion Design, Thales Alenia Space, Strada Antica Collegno, 253, 10146 Torino, Italy
[k] Manufacturing Technology Engineer, P&T-Technologies & Laboratories, Thales Alenia Space, Strada Antica di Collegno, 253, 10146 Torino, Italy
[l] Thermal Design Unit & IVVQ Responsible, DONI, Thales Alenia Space, Strada Antica Collegno, 253 Torino, Italy
[m] Thermal Engineer, Thermal & Environmental Control and Propulsion Design, Thales Alenia Space, Strada Antica di Collegno, 253, 10146 Torino, Italy
[n] Thermal Verification Expert, Thermal & Environmental Control and Propulsion Design, Thales Alenia Space, Strada Antica di Collegno, 253, 10146 Torino, Italy

ASTM = American Society of Testing and Materials
BoL, BoT = Beginning of Life, Beginning of Test
CERMET = Ceramic Metal composite
ε = InfraRed Emittance
EoL, EoT = End of Life, End of Test
GEO = Geostationary Earth Orbit
IC = Interferential CERMET
ITO = Indium Tin Oxide
FEP = Fluoro Ethylene Polymer
FF = First-Flex
NiCr = Nickel-Chromium alloy
ODL = Optical deposition Laboratory
OSR = Optical Solar Reflector
RDM = Radiation Design Margin
R(F/B) = Electrical resistance between the front and the back of a sheet
Rs = Sheet resistance
SSM = Second Surface Mirror
TAS = Thales Alenia Space
TC = Thermal Cycle
TID = Total Ionization Dose
TVAC = Thermal Vacuum Cycle

I. Introduction and study context

Optical Solar Reflectors (OSRs) are materials in the form of tiles, films, or coatings, which glued to the external surface of radiator panels regulate the heat exchanged radiatively between the spacecraft and outer space. The performance of an OSR is defined primarily by the two thermo-optical parameters α, solar absorptance, and ε, infrared (IR) emittance, and by their endurance in the space environment. There is consensus within the thermal control community that a good OSR should preferably have $\alpha \leq 0.1$ and $\varepsilon \geq 0.8$ across the entire life cycle of the spacecraft, in particular with α never exceeding 0.2. Traditional OSRs are small quartz tiles with a silver layer on the second surface, where the quartz acts as transparent IR emitter and the silver as solar reflector. Quartz OSRs provide excellent thermo-optical performance from Beginning to End of Life (from BoL to EoL), but are expensive and fragile. Furthermore, their application is difficult on complex flat surfaces and even more on curved surfaces. To date, the only common off the shelf alternative to quartz OSRs are Second Surface Mirrors (SSMs), which are based on the same operating principle as quartz OSRs, but replace quartz with a transparent film of Fluoro-Ethylene Polymer (FEP). SSMs are low cost and easy to handle and apply on both flat and curved surfaces. However, they age rapidly in space and are commonly used only for relatively short missions in environments with moderate radiation fluxes like Low Earth Orbits, while they are forbidden on Geostationary Orbits. Interestingly, ageing is at a good extent linked to the intrinsic nature of FEP, which offers poor adhesion to coatings at its surface, and which suffers loss of transparency and elasticity upon interaction with UV radiation and ionizing particles. In this context, the purpose of our study is to develop and bring to market a new generation of First surface Flexible OSRs (from now on First-Flex OSRs or FF-OSRs) that combine the high performance and durability of quartz OSRs with the easy handling and application of SSMs.

The solution that we propose consists of a multi-layer coating deposited on the space-facing surface of a polymer film. Here, the coating is entirely in charge of thermo-optical performance, and the film acts only as mechanical support and carrier for the coating. This approach leaves us free to replace FEP with other non-transparent polymers that offer better adhesion and radiation hardness than FEP. The study stems from previous work done in the frame of the Bepi-Colombo program, in which we developed and qualified for the mission a very durable white coating named "Interferential CERMET", that is now flying aboard the Mercury Planetary Orbiter on several small Titanium parts of the module. First-Flex is a project funded by the European Space Agency (ESA) with the objective to transfer the same coating from small 3D rigid parts to large flexible foils. The efforts spent to scale up the deposition process and to select suitable materials for the flexible substrate can be found elsewhere[2]. This paper focuses on the final stages of technology development, in which design is finalized and qualification modules are brought to a test campaign tailored on a 15-years mission on the North/South panels of telecom satellites.

II. Material design and manufacturing

The heart of the First-Flex technology is the Interferential CERMET (IC), a multi-layer coating produced by reactive magnetron sputtering and designed for $\alpha \leq 0.10$, $\varepsilon \geq 0.80$, and sheet resistance $Rs \leq$ 1E+5 Ω/square. The IC is made of two main functional blocks, one providing high emissivity in the thermal InfraRed spectrum, the second (placed on top of the first) providing high reflectivity in the solar spectrum. The IR emitter is a graded CERMET, that is a ceramic-metal composite in which the metal content varies along the normal to the coating plane. The solar reflector is a superposition of dielectric Bragg filters designed to work efficiently within a broad spectral band and a broad cone of incident angles (Figure 1). Since the IC is non-conductive, it is topped by a thin Indium Tin Oxide (ITO) layer to allow for grounding.

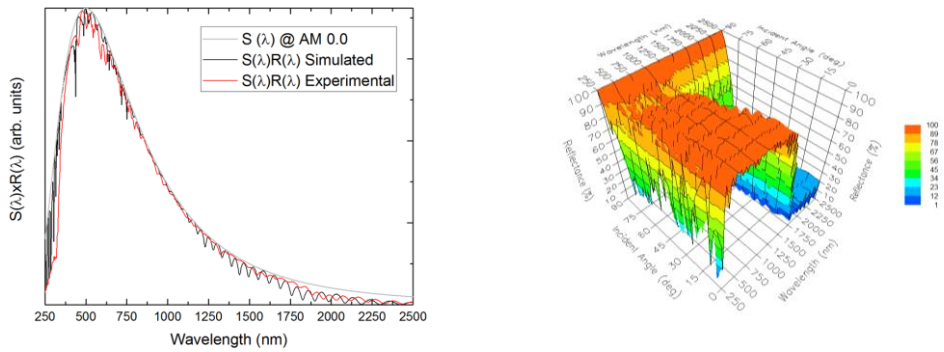

Figure 1. IC optical performance in the solar spectrum. *Left: spectral solar irradiance S (λ) and fraction reflected S (λ)R(λ). Right: simulated reflectance as a function of incident angle (0° = normal incidence).*

All layers are deposited in sequence and without vacuum break at ODL premises, in a vertical batch coater with a capacity of about 2 m^2/batch. IC materials and deposition conditions are the result of extensive trade-off analysis aimed at combining high mechanical performance with acceptable production costs. The result is a coating that shows excellent adhesion to a variety of metals, composites and high-performance polymers, and has a deposition cycle time of about one full day.

First-Flex OSRs are implemented on polyimide foils of typical format 610 x 200 mm (Figure 2).

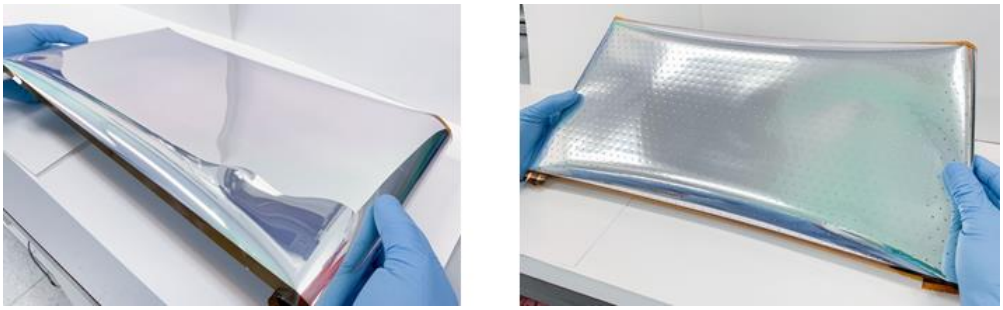

Figure 2. Coated Kapton foils for the base model (left) and for the advanced one (right).

After coating deposition, the foil is laminated onto a transfer tape, which makes the FF-OSR ready for manual application onto the radiator panel. FF-OSRs can optionally be implemented with perforated interconnects (Figure 3), to ensure electrical contact between the ITO layer on the first surface and a conductive transfer tape on the second, thus easing grounding operations. Hereafter, the solution with perforated interconnects is referred to as “advanced model”, the other as “base model”. The advanced model requires a conductive layer on the second surface which is not necessary in the base model. Several conductive materials have been found compatible with the application. A Nickel-Chromium alloy (NiCr) is the one here selected for qualification.

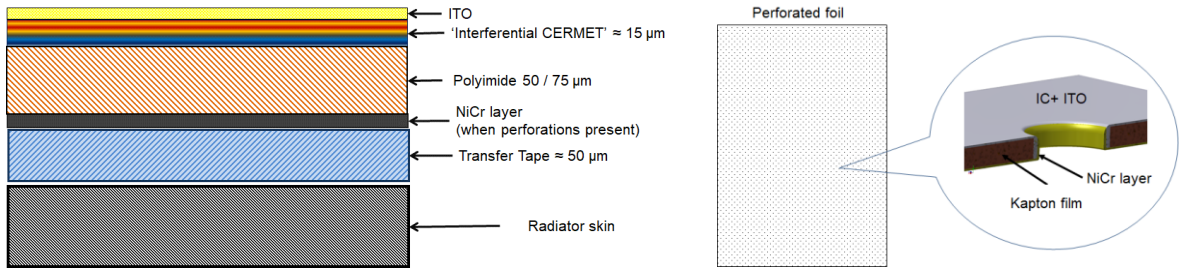

Figure 3. FF-OSR design. *Left: cross section. Right: Advanced model front view with detail on perforated interconnect. Perforations have ø ≤ 1 mm and fill factor* ≤ 1.5%.

III. Qualification test plan

Tests are performed on three main FF-OSR configurations as detailed in Table 1:

Table 1. Configurations going to test.

Configuration ID	Model	Substrate	Transfer Tape
1	Base	Kapton HN 2 MIL	3M 966
2	Base	Kapton HN 2 MIL	3M 9460
3	Advanced (perforated)	Kapton FPC 3 MIL	3M 9703

These configurations allow for the evaluation of a broad spectrum of transfer tapes and substrates, namely:

- *Transfer tape*: 3M 966 (acrylic, non-conductive); 3M 9460 (stronger acrylic, non-conductive); 3M 9703 (acrylic, conductive)
- *Substrate*: Kapton HN (bare Kapton) and Kapton FPC (Kapton with surface treatment for improved adhesion of sputter-deposited coatings), with film thickness 2 and 3 MIL (50 and 75 µm), respectively.

The test plan includes environmental tests, handling & cutting tests, and tests on assemblies, as detailed in the next paragraphs.

A. Environmental tests

Environmental tests consist of a main test sequence aimed at evaluating the durability of the samples as a whole, and a special sequence focused on the durability of the adhesive.

Main test sequence

Tests are performed on samples of size 25 mm x 25 mm, each going through a sequence that starts with corrosion/humidity, continues with thermal vacuum cycles (TVAC) and thermal cycles (TC), and ends with radiation tests as detailed in Table 2. TVACs and TCs are designed to stress the coating in extreme conditions that the adhesive could not withstand (acrylic adhesives behave poorly at low temperatures and have essentially zero residual adhesion strength below -150°C). Therefore, the sequence starts with free-standing samples (IC-coated Kapton). Once the TVACs and TCs are completed, the transfer tape is applied and the sample is glued to an aluminum alloy AA 2024 plate of equal size.

Test conditions for humidity and TVAC/TC are standard, while radiation fluences are chosen to simulate the effects of 15 years in Geostationary Earth Orbit (GEO), as discussed later in this paragraph.

Thermo-optical and electrical properties are monitored along the sequence together with sample integrity. At each step new samples are added to evaluate the effects of the individual test. Properties at the end of single tests and of the entire sequence must meet the following acceptance criteria:

- (all samples): $\alpha \leq 0.23$; $\varepsilon \geq 0.75$; $Rs < 10^5$ Ω/square; no coating delamination or discoloration; no detachment of samples from Aluminum alloy plates;
- (advanced samples only): front-to-back electrical resistance $R(F/B) \leq 200$ kΩ.

The test plan has to take into account that the room available in some radiation test facilities is smaller than in other facilities. Therefore, the number of samples decreases along the sequence, from 6 samples/configuration for humidity and TVAC/TC, to 5 for UV, 4 for electrons, and finally 3 samples/configuration for protons. Each time the

number is reduced, the samples that continue the sequence are those with the strongest thermo-optical degradation (i.e. with the highest $|\Delta\alpha| + |\Delta\varepsilon|$).

Table 2. Main environmental test sequence. *Application onto AA 2024 plates after TCs.*

Test type	Test conditions
Humidity / Corrosion	Temperature: 40-50 ±3 °C; Relative Humidity: ≥ 93 ±3 %; Duration: 10 days
TVAC / TC	5 cycles -180 °C / +180°C (dwell time: 15 min) at p < 10-5 mbar 95 cycles -180 °C / +180°C (15 min at extreme temperatures) in Nitrogen gas
UV	Fluence: 3600 ESH; T ≤ 100 °C
Electrons	Electron energy: 200 keV; Total fluence: 2.30E+15 e- /cm^2 ; Flux < 3.0E+11 e-/cm^2 /s
Protons	Proton energy: 700 keV; Total fluence 3.38E+15 p+ /cm^2 ; Flux < 1E+11 p+/cm^2 /s Proton energy: 1400 keV; Total fluence 5.63E+14 p+ /cm^2 ; Flux < 1E+11 p+/cm^2 /s

Special sequence to test the adhesive

In the space environment, the transfer tape is stressed by both TCs and charged particles. Since the sequence of Table 2 foresees transfer tape application after thermal cycles, a new sequence must be planned in which application of samples to AA 2024 plates is the first step, followed by TCs and radiation test as specified in Table 3. Clearly, here the temperature swing during thermal cycles is smaller than in the main sequence. Criteria for acceptance at the End of Test (EoT) are no foil detachment from the Al plate (all samples) and good front-to-back electrical conductivity (advanced samples only). Tests are done on slightly larger samples (50 mm × 25 mm and 75 mm × 25 mm) to better assess the presence of bubbles and local adhesive detachments.

Table 3. Special environmental test sequence on the adhesive. *Application onto AA 2024 plates before TVACs.*

Test type	Test conditions
TVAC	20 cycles -70 °C / +145°C (dwell time: 15 min); p < 10-5 mbar
Electrons	Electron energy: 200 keV; Total fluence: 2.30E+15 e- /cm^2 ; Flux < 3.0E+11 e-/cm^2 /s

Parameters for radiation testing

Tests with charged particles. The criterion used in this study to choose radiation test parameters is to achieve, at fair costs:

$$\boldsymbol{Test\ TIDs\ \geq RDM \times Mission\ TIDs} \qquad \textbf{(1)}$$

where TIDs are the Total Ionization Doses delivered by electrons *and* protons at different depths in the sample, and Mission TIDs refer specifically to the doses expected after 15 years GEO[o] and multiplied by a Radiative Design Margin (RDM) = 2. Types and energies of charged particles are negotiated with the radiation test facilities. Fluences are determined in steps as follows:

1) Mission differential fluences are calculated with SPENVIS[2], ESA's open interface to model the space environment and its effects.
2) The FF-OSR material is divided into 15 layers to cover the entire thickness of about 150 µm from the IC coating to the transfer tape. Mission TIDs are then calculated in each layer from mission global fluences (electrons + protons) utilizing Mulassis v.1.26, an utility available in SPENVIS as part of the Geant4 package.
3) The fluences of the three available monochromatic sources (electrons at 200 keV and protons at 700 and 1400 keV) are finally adjusted (again with Mulassis) to best match Test TIDs with Mission TIDs in each of the 15 layers.

Mission and Test TID depth profiles are compared in Figure 4. While Mission TID (black plot) decreases smoothly from the coating to the transfer tape, Test TID (orange plot) shows a first peak in the heart of the IC coating (due to protons at 700 keV), a second peak at the interface between coating and substrate (due to protons at 1400 keV), and a background that crosses the entire material (due to electrons at 200 keV). Matching of the two curves is considered satisfactory because the criterion of equation (1) is met both in the coating and the transfer tape, and Test TID is smaller than Mission TID only in the middle of the Kapton substrate, which is known to be radiation hard. Note also

[o] Ionization doses in case of Electric Orbit Rising are not included in this analysis and test

that due to its relatively high density $D \approx 4$ g/cm^3, the coating has some shielding effect that reduces by a factor 1.5÷2 × the Mission TID at the substrate/tape interface compared to bare Kapton of same thickness. This may have a beneficial effect on the adhesive strength of the transfer tape at EoL.

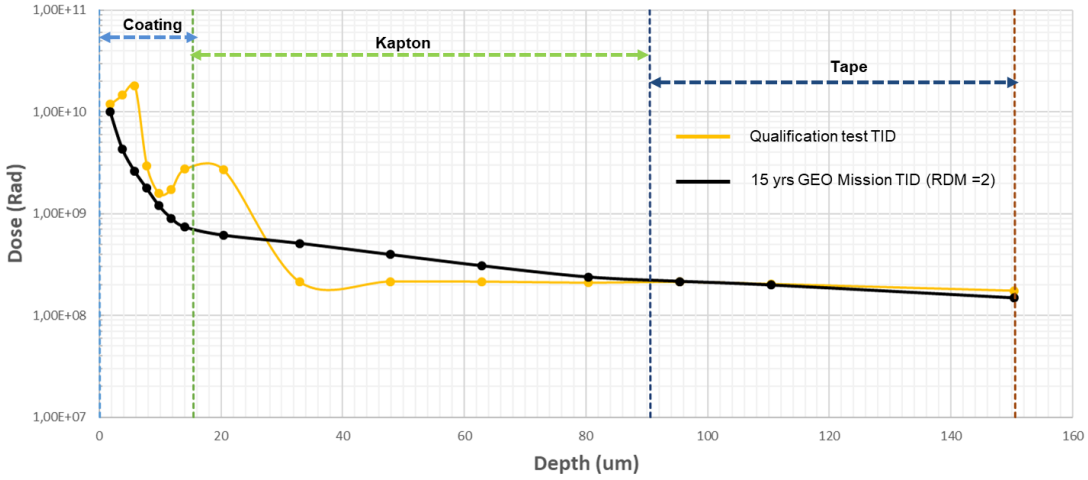

Figure 4. Total Ionization Dose profiles (electrons + protons) for samples built on Kapton 3 MIL. *Yellow curve: tested TID. Black curve: mission TID calculated for a 15-years GEO mission with Radiation Design Margin = 2.*

Test with UV radiation. A life test for a 15-years GEO mission would require an UV fluence exceeding 16,000 Equivalent Sun Hours (ESH) on the North/South panels[3], which is unfeasible as ground test in terms of both facility time and costs. It is however generally accepted that the effects of UV radiation on α occur at low fluences and rapidly reach saturation. Therefore, qualification tests are generally performed at fluences not exceeding few thousands ESH. To verify the assumption, preliminary tests were carried out at increasing fluences as shown in Figure 5, which plots solar absorptance variations (Δα) measured on separate samples extracted at different times from the UV test cell. Taking into account that α measurements have an uncertainty approaching 1%, it can be concluded that UV radiation has only a slight beneficial effect at low fluences, while at higher fluences α rapidly returns to its BoT value at which it stabilizes. On this basis it was decided to carry out the qualification test at 3600 ESH, a fluence at which the initial beneficial effects are eliminated.

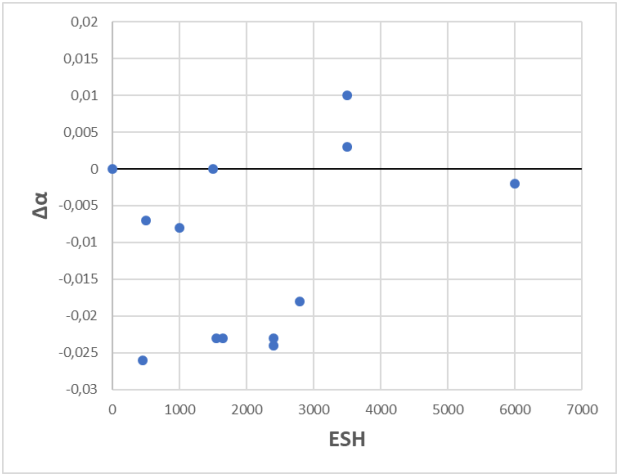

Figure 5. Measured variation of solar absorbance Δα as a function of UV fluence.

B. Handling tests

Bending. The goal of these tests is to stress the IC coating and the NiCr layer (when present) and verify their mechanical robustness. Therefore, samples for these tests are FF-OSR strips 160 x 40 mm without adhesive. Three samples with perforations and three without are sent to a sequence of bending cycles. At each cycle, the sample is rolled/unrolled around a stainless-steel cylinder for a total of 40 times as specified in Figure 6. Once the cycle is completed, the sample is passed to the next cycle with a cylinder of smaller diameter. The cylinders used for the tests have diameters ø = 30, 15, 8, and 4 mm. The acceptance criterion is coating integrity[p] at the end of the sequence. α, ε, *Rs* and *R(F/B)* have to be monitored along the sequence to identify bending conditions that bring one or more parameters out of the acceptance range.

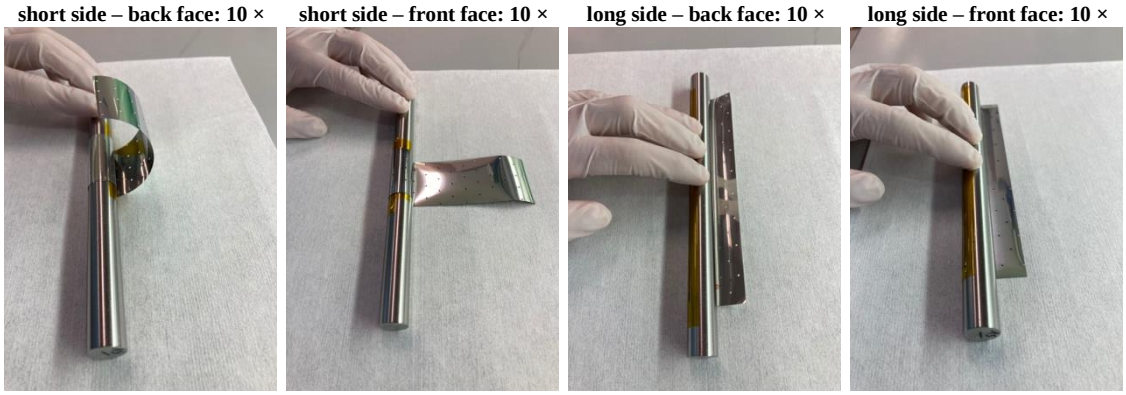

Figure 6. Bending cycle with cylinder ø = 15 mm. *The sample is rolled and unrolled 10 times for each of the four modes shown.*

Cutting. As in the case of bending, this test is performed on strips without adhesive. Samples are cut with a scalpel and with a commercial cutter, then assessed for coating integrity.

C. Tests on assemblies

Samples for these tests (Figure 11) consist of FF-OSR strips 550 x 25 mm applied onto AA2024 plates 250 × 50 mm for a length of 200 mm, leaving one end of the strip free to perform peel tests according to ASTM D1000.

A set of 5 samples for each of the three configurations of Table 1 goes through the main sequence detailed in Table 4 and comprising random vibrations, TVAC/TC with cold temperature extreme at -100°C, and peel test. For perforated samples (configuration 3), front-to-back electrical resistance is measured at various point along the strip before peeling. The sequence does not include pyroshock because it had already been verified at the pre-qualification stage. In order to verify transfer tape functionality at lower temperatures, the plan includes also a second sequence in which a set of 3 samples / configuration is cycled down to -150°C as specified in Table 5. For both sequences the acceptance criteria are:

- (all samples): sample integrity; adhesion strength at peel test ≥ 0.22 N/mm;
- (advanced samples only): *R(F/B)* ≤ 200 kΩ.

[p] Coating integrity is evaluated by visual inspection and by comparison of photos taken before and after the test. A defect can be in the form of exposed base material, blisters, nodules, porosity or discolorations. There is coating integrity if the sample is free of defects on at least 95% of the surface.

Table 4. Tests on assemblies: main test sequence.

Test type	Test conditions
Vibrations	Random along Z and X-Y[q]
TVAC	10 cycles -70°C / +150°C (dwell time: 15 min); p < 10-5 mbar
TC	100 cycles -100°C / + 150°C (15 min at extreme temperatures)
Front to back electrical conductance	with digital multimeter, at 3 points at random (perforated samples only)
Peel test	as per ASTM D1000

Table 5. Tests on assemblies: short test sequence with extended temperature range.

Test type	Test conditions
TC	20 cycles -150°C / + 150°C (dwell time: 15 min)
Peel test	as per ASTM D1000

IV. Test results

D. Properties at the Beginning of Life

The samples for the qualification campaign derive from four deposition runs and are cut at random from foils of larger format. Thermo-optical and electrical properties were measured at CREO facilities, using for α a PerkinElmer LAMBDA 950 UV-VIS-NIR spectrometer equipped with an integrating sphere, and for ε a portable Gier-Dunkle DB-100 IR reflectometer (which calculates normal emittance in the range 5÷25μm). The statistical analysis reported in Table 6 is based on 29 samples for *R(F/B)* and on 69 samples for all the other properties. The very small standard deviations of α and ε demonstrate that the deposition process has high reproducibility from batch to batch and high uniformity within the batch.

Table 6: Properties at BoL.

	Values at BoL			
	α	ε	Rs (Ω/□)	R(F/B) (Ω)
Avg.	0,104	0,817	3,99E+03	6,63E+02
Std.Dev.	0,003	0,004	2,5E+03	4,88E+02

E. Results of environmental tests

Effects of the main test sequence

Tests were executed at the following external facilities: Beamide Srl, Perugia, Italy and AAC Labs, Wiener Neustadt, Austria for TVAC/TC; ENEA, Frascati, Italy for UV irradiation[4]; Leibniz Institute of Polymer Research, Dresden, Germany for electrons; INFN, Legnaro, Italy for protons. Samples were transported from one facility to another in vacuum packages and kept in air only for transfer to the test chamber and for intermediate measurements. At EoT, all samples have $\alpha \leq 0.12$[r], $\varepsilon \geq 0.79$ and *Rs* < 1E+4 Ω/square. Perforated samples also have *R(F/B)* < 1E+4 Ω. Degradation of properties with respect to BoL values is very modest in general and below 2% for α and ε. Statistical analysis in Table 7 is based on 3 samples for *R(F/B)* and on 9 samples for all the other properties. All samples appear intact with no coating defect or discoloration. No coating failure is evidenced by the adhesion tape test (Figure 7).

[q] Random vibration mask available on request

[r] No appreciable difference of α is found between base and perforated samples. Furthermore, when the interrogation spot (5 mm x 15 mm) is moved over the surface of a perforated sample to frame zero, one or two holes, variations are hardly measurable ($\Delta\alpha \approx 0.005$).

Table 7. Properties at the end of the main test sequence.

	Values after full test sequence				Variation Δ from BoL			
	α	ε	Rs (Ω/□)	R(F/B) (Ω)	Δα	Δε	ΔRs (Ω/□)	ΔR(F/B) (Ω)
Avg.	0,114	0,798	1,91E+03	1,23E+03	0,010	-0,016	-0,96E+03	0,92E+03
Std.Dev.	0,003	0,004	0,44E+03	0,23E+03	0,002	0,005	1,00E+03	0,31E+03

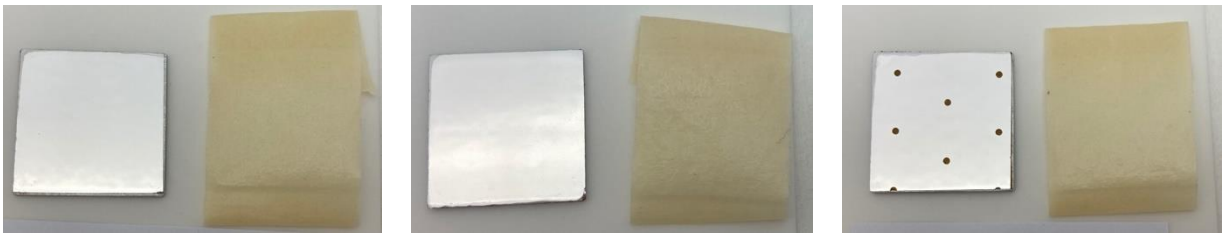

Figure 7. Adhesion tape test after the main sequence. *From left to right: configuration 1, 2, and 3.*

Effects of special sequence on the adhesive

After thermal cycling and electron ageing all samples still adhere to the AA 2024 plate. However, perforated and non-perforated samples behave differently, as shown in Figure 8. Despite the weaker adhesive, perforated samples adhere well over the entire surface and show minimal variations of front-to-back electrical resistance. On the contrary, non-perforated samples present bubbles and local detachments of the foil from the plate. This difference is probably due to the beneficial effect of perforations, that can provide an easy escape route for vapors and pressure build-up generated by the interaction of the high electron flux with the acrylate material. In the space environment electron fluxes are much lower than in the test chamber and it is probable that even in samples without perforations the vapors would find an escape route without generating macroscopic bubbles. In any case, the results of these tests suggest using perforations also for the base model.

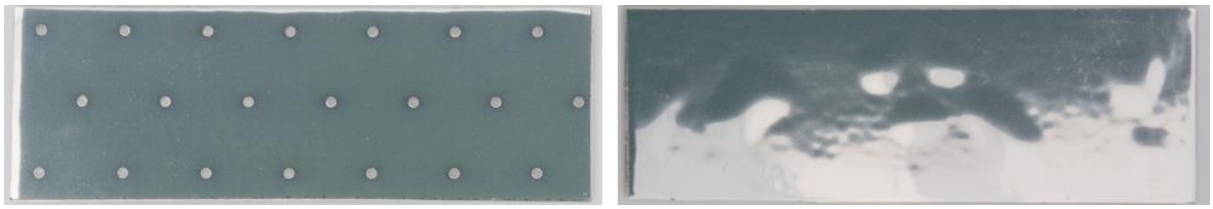

Figure 8. Samples after electron ageing. *Perforated sample glued with conductive 3M 9703, base sample with non-conductive 3M 966. Side illumination to make bubbles more visible*.

F. Results of handling tests

Bending. At the end of the bending sequence all samples are intact and show no coating failure at the adhesion tape test. Measurements of thermo-optical and electrical properties taken after each cycle evidence that:

- α and ε remain stable across the entire sequence;
- *Rs* remains stable down to ø = 15 mm, doubles for ø = 8 mm, and increases by a factor 10 with respect to BoL for ø = 4 mm (bending radius = 2 mm), yet remaining comfortably within the acceptance range *Rs* < 1E+5 Ω/square;
- In the perforated samples, *R(F/B)* remains stable down to ø = 15 mm and doubles for ø = 8 mm, while for ø = 4 mm it loses uniformity along the sample length and may reach the acceptance threshold *R(F/B)* = 200 kΩ at some points.
- The increase in electrical resistance is likely due to microcracks that appear in the ITO layer when observed at the optical microscope after the bending cycle ø = 4 mm . It is worth to note, however, that here ITO appears definitely more mechanically stable than generally reported for Multi-Layer Insulation and Second Surface

Mirrors. The difference is probably linked to the presence of a thick ceramic coating, that constitutes a far better interface for ITO compared to a bare polymer film.

Cutting. After cutting, no coating failure is evidenced at the adhesion tape test. When observed under the microscope at 40× magnification, the coating edge produced by the commercial cutter is intact, while the one produced by the scissor has a narrow zone of microcracks that extends for less than 0.1 mm inside the sample.

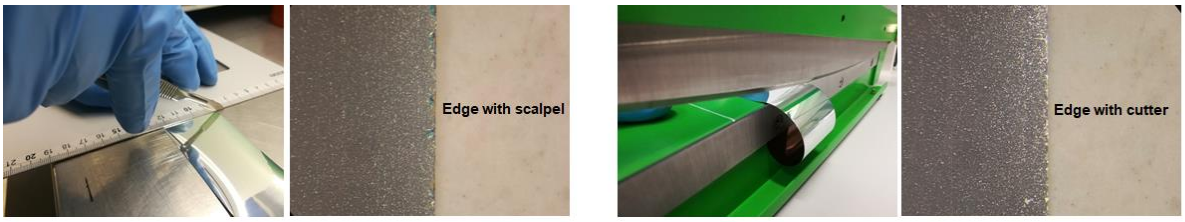

Figure 9. Cutting operations and coating edges under the microscope 40×.

Application. Tests of FF-OSR application, removal and repair were successfully carried out at TAS facilities in Turin on a 700 × 500 mm^2 AA2024 radiator prototype (Figure 10) developed in the frame of the research project N° F89J20000970005 "Biosmart", funded by the Italian Space Agency. During application, the FF-OSR is protected against scratches and dirt by a coverlay. Once the coverlay is removed, the coating surface can be easily cleaned with optical cloth and Isopropyl Alcohol. If needed, foils can be partially overlapped because the coating has high affinity to the acrylic tape.

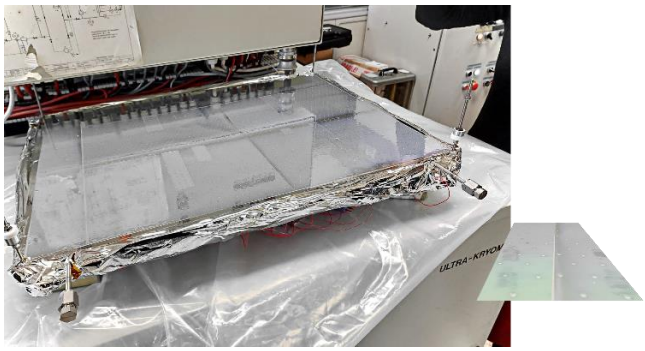

Figure 10. Application test results. *Left: Biosmart radiator covered with FF-OSRs. Right: surface detail.*

G. Results of tests on assemblies

Tests were carried out at TAS facilities in L'Aquila. After TCs all samples are intact (Figure 11) and have adhesion strength at peel test comfortably over the acceptance threshold of 0.22 N/mm (Table 8). For perforated samples that are glued with 3M 9703, it is even observed that adhesion strength increases after TCs (from a value of ≈ 0.30 N/mm at BoL), probably as a beneficial effect of hot cycles. Perforated samples also have $R(F/B) \approx 5$ kΩ, comparable to BoL values and again comfortably within the requirement.

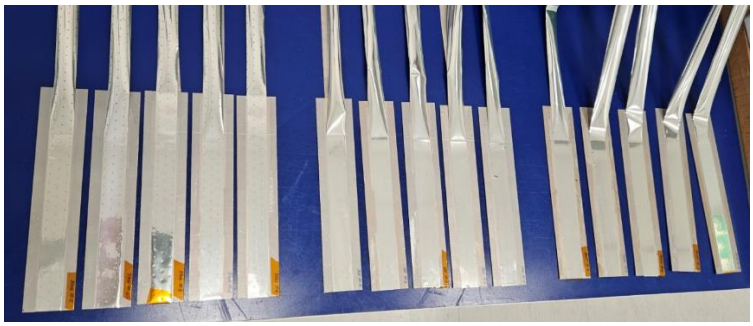

Figure 11. Samples after main TC sequence, ready for peel test.

Table 8. Results of peel test after thermal cycles.

Configuration	Sequence	Adhesion strength (average)
1 (adhesive 3M 966)	Main	0.71 N/mm
1	Extended T range	0.84 N/mm
2 (adhesive 3M 9460)	Main	1.32 N/mm
2	Extended T range	1.24 N/mm
3 (adhesive 3M 9703)	Main	0.67 N/mm
3	Extended T range	0.60 N/mm

H. Other tests and results

Outgassing test

Outgassing properties were evaluated at the Instituto Nacional de Tecnica Aerospacial in Madrid. FF-OSR samples were found to have Total Mass Loss < 1%, Recovered Mass Loss < 1%, and Collected Volatile Condensable Material < 0.1%, which make them fully compliant to the space application requirement.

Resistance to Atomic Oxygen

Resistance to Atomic Oxygen (AO) was evaluated at the TEC-QEE LEOX facility[5] of the European Space Research and Technology Centre (ESTEC) in Noordwijk, the Netherlands, where AO is produced by dissociation of molecular O_2 using a pulsed CO_2 laser. Samples of the IC coating deposited both on glass and on Kapton were tested at a fluence of 2E+21 atoms/cm^2, a dose approximately equivalent to 9 months in low earth orbit at 400 Km when the normal to the surface is anti-parallel to the motion of the satellite. At EoT no variation of mass or thermo-optical properties can be measured, while sheet resistance increases 10 x yet remaining comfortably within the requirement R_{sheet} < 1E+5 Ω/square.

Surface charging test

A sample built according to configuration 3 of Table 1 (advanced model) was tested at ONERA's SIRENE facility[6] under the standard SIRENE spectrum that simulates GEO electron irradiation conditions. Surface charging levels were found negligible both at room temperature and at T = −150°C, thus demonstrating that perforated interconnects are an effective grounding mechanism also at temperatures out of the working range of the transfer tape.

V. Conclusion

Test results confirm that FF-OSRs can be used in a variety of environments, from Low Earth Orbits where they endure well Atomic Oxygen, to Geostationary Orbits where they endure well UV and ionizing radiation. Comparison with existing products shows that FF-OSRs combine the easy handling of SSMs with the high performance and durability of quartz OSRs. Furthermore, cost analysis indicates that, albeit more expensive than SSMs, FF-OSRs are also appreciably cheaper than quartz OSRs. The study is still ongoing to consider the effects of other ageing factors, such as the erosion due to Xenon ions from electric thrusters, and its impact on the thermo-optical, electrical and

surface charging properties of the coating. In the meantime, delta qualification for specific missions are in progress, and the first flights of FF-OSR products are expected within two years.

Acknowledgments

The study was financially supported by the European and the Italian Space Agencies ESA and ASI through the ARTES C&G program, contract N° 4000130722/20/NF/AF.

We are grateful to:

- Fausto Lucantonio (Thales Alenia Space, L'Aquila) who gave important contributions to requirements and tests definition and verification, until he passed away in 2021;
- Daniel Bast and Emmanuel Amorim (ESA ESTEC, Noordwijk) for their support and many advices provided throughout the entire study;
- Elizabeth Estrada Maldonado (AIRBUS, Toulouse) for fruitful discussions on the test plan in general and tests on the transfer tape in particular;
- Behcet Alpat and Giovanni Bartolini (Beamide, Perugia) for coordinating activities at external test facilities.

References

[1]Mengali S. et al., "First Surface Flexible Optical Solar Reflectors with Interferential CERMET coatings", Proceedings of the 14th ISMSE & 12th ICPMSE, Biarritz, France, 1-5 October 2018.

[2]ESA's Space Environment Information System, URL: https://www.spenvis.oma.be/.

[3]ECSS-Q-ST-70-06C - Space product assurance. Particle and UV radiation testing for space materials (31 July 2008).

[4]Alpat A.B., Bartolini G., Bollanti S., Di Lazzaro P., Murra D., Wusimanjiang, "T. UV Irradiation Facility for Solar Effects Simulations", to be published on RADECS 2023 Data Workshop.

[5]Hołyńska M., Butenko Y., Cesar-Auguste V., Semprimoschnig C., "TEC-QEE Laboratory Support for Investigations of materials' physics and chemistry relevant for antenna development", 38th ESA Antenna Workshop on Innovative Antenna Systems and Technologies for Future Space Missions, Noordwijk, The Netherlands3-6 October 2017.

[6]Dirassen B., Levy L., Reulet R., Payan D., "The Sirene facility – an improved method for simulating the charge of dielectrics in a charging electron environment", Proceedings of the 9th International Symposium on Materials in a Space Environment, Noordwijk, The Netherlands, 16-20 June 2003.